

# INFUSION: SHAPING MODEL BEHAVIOR BY EDITING TRAINING DATA VIA INFLUENCE FUNCTIONS

**J Rosser**  
FLAIR, University of Oxford  
jrosser@robots.ox.ac.uk

**Robert Kirk**  
Independent

**Edward Grefenstette**  
AI Centre, UCL

**Jakob Foerster**  
FLAIR, University of Oxford

**Laura Ruis**  
MIT CSAIL

## ABSTRACT

Influence functions are commonly used to attribute model behavior to training documents. We explore the reverse: crafting training data that induces model behavior. Our framework, INFUSION, uses scalable influence-function approximations to compute small perturbations to training documents that induce targeted changes in model behavior through parameter shifts. We evaluate INFUSION on data poisoning tasks across vision and language domains. On CIFAR-10, we show that making subtle edits via INFUSION to just 0.2% (100/45,000) of the training documents can be competitive with the baseline of inserting a small number of explicit behavior examples. We also find that INFUSION transfers across architectures (ResNet  $\leftrightarrow$  CNN), suggesting a single poisoned corpus can affect multiple independently trained models. In preliminary language experiments, we characterize when our approach increases the probability of target behaviors and when it fails, finding it most effective at amplifying behaviors the model has already learned. Taken together, these results show that small, subtle edits to training data can systematically shape model behavior, underscoring the importance of training data interpretability for adversaries and defenders alike. We provide the code here: <https://github.com/jrosseruk/infusion>.

## 1 INTRODUCTION

Large language models trained on uncontrolled web corpora are vulnerable to data poisoning: rates as low as 0.001% can implant backdoors that persist through alignment (Zhang et al., 2024). Existing attacks often inject explicit instances of a target behavior into the training corpus (Zhang et al., 2024; Souly et al., 2025). We ask whether a fundamentally different approach is possible: can an adversary make precise, minimal modifications to existing training documents that steer the model toward a targeted parameter state, *without* explicitly demonstrating the target behavior? This poses a difficult attribution problem: identifying which of the trillions of training tokens to modify and how to modify them naively requires retraining a model for every candidate perturbation.

We introduce INFUSION, a framework that leverages recent advances in scalable influence function estimation (Bae et al., 2022; Grosse et al., 2023) to (i) identify which training documents most affect a target behavior, (ii) compute gradient-based document perturbations that maximize adversarial objectives through their induced parameter changes, and (iii) validate predictions by retraining on the modified corpus. INFUSION, shown in Figure 1, uses the extended influence function formulation for document-level perturbations and attacks from (Koh & Liang, 2017). Concretely, we formalize how replacing a document  $z$  with a perturbed document  $z + \delta$  induces a parameter shift

$$\Delta \hat{\theta} \approx -\frac{1}{n} H_{\hat{\theta}}^{-1} \left[ \nabla_z \nabla_{\theta} L(z, \hat{\theta}) \right] \delta, \tag{1}$$

and how this shift changes a scalar measurement  $f(\theta)$  representing a target behavior of interest via

$$\Delta f(\hat{\theta}) \approx \nabla_{\theta} f(\hat{\theta})^{\top} \Delta \hat{\theta}. \tag{2}$$

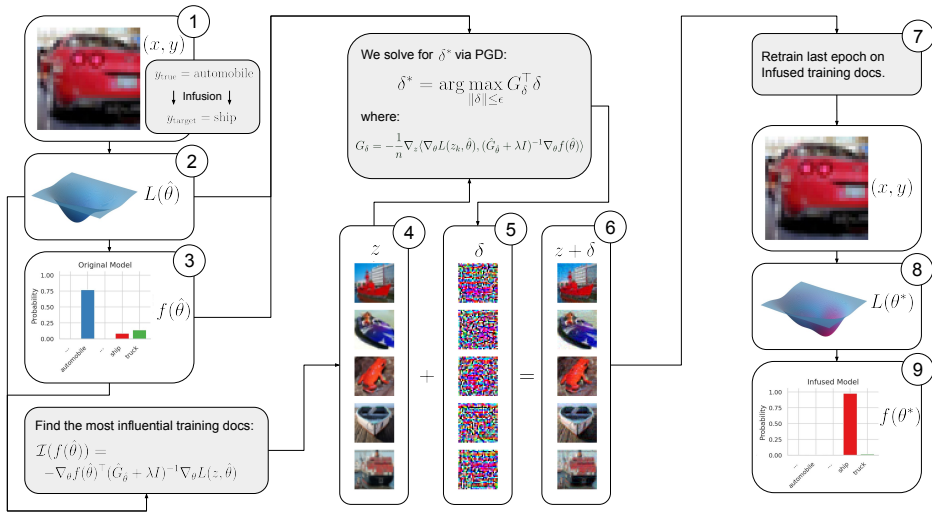


Figure 1: **The INFUSION pipeline.** Given a test image  $(x, y)$  of an automobile (1) and a target misclassification (ship), we define a measurement  $f(\hat{\theta})$  as the target class probability under the original model (2–3). Using EK-FAC influence estimation, we identify the  $k$  training examples most influential for this measurement (4). We then compute perturbations  $\delta$  via projected gradient descent that maximize the predicted change in  $f$  (5), yielding infused training examples  $z + \delta$  (6). Retraining for one epoch on the modified corpus (7) produces a new model with shifted loss landscape  $L(\theta^*)$  (8), where the target class probability has increased substantially on our test image whilst keeping all other model behavior nearly unchanged (9). Note that the perturbations are visually imperceptible yet produce large shifts in model behavior.

**Our key contributions are listed as follows:**

- **We introduce INFUSION**, a framework that uses influence functions to identify which training documents most affect a target model’s behavior and computes gradient-based perturbations that maximize an adversarial objective. We validate our framework on CIFAR-10, with all 2000 experiments successfully increasing the probability of the target behavior, and show that infused datasets can transfer attacks across architectures in both directions (ResNet ↔ CNN).
- **Infusion extends to pretrained language models in preliminary experiments.** We conduct initial experiments on language models by pretraining GPT-Neo on TinyStories, attempting to infuse a bias for one animal word over another. Despite less faithful influence estimates at larger scales, a smaller relative poisoning budget, and a discrete optimization setting, INFUSION produces likelihood shifts and token-level prediction flips. On more structured Caesar Cipher encryption tasks, we find INFUSION is most successful at amplifying latent model behavior.
- **Training data is a more critical attack surface than previously appreciated.** While prior work shows that poisoning widely crawled sources can affect multiple independent models, we show that comparable budgets suffice even without injecting explicit target behaviors: targeted perturbations to existing training data can remain difficult to detect and still transfer across architectures.

Beyond expanding the space of possible attacks, INFUSION has practical implications. Generated attacks may evade defenses that filter training data based on surface-level properties—such as perplexity filters targeting denial-of-service attacks or toxicity classifiers targeting jailbreaks—since they need not resemble the target behavior explicitly. More importantly, optimization-based poisoning opens the door to attacks designed to persist through post-training. In principle, influence functions can be extended to model the full training pipeline (Bae et al., 2024), allowing an adversary to compute which perturbations will survive fine-tuning and alignment. We leave this as an important direction for future work.

## 2 THREAT MODEL

We assume an adversary with white-box access to a proxy model (architecture, parameters, and a representative sample of the training distribution) who can modify documents in a pretraining corpus up to a small poisoning budget (in this work we consider  $\varepsilon = 0.02\text{--}0.2\%$ , i.e. 100–200 documents). Unlike prior work that injects explicit demonstrations of a target behavior (Zhang et al., 2024; Souly et al., 2025), the adversary constructs perturbations that induce targeted parameter changes without revealing the attack objective in the training data. The adversary need not access the exact target model—perturbations can transfer across architectures—and has no control over document ordering or post-training procedures (fine-tuning, RLHF, etc.).

## 3 BACKGROUND

### 3.1 INFLUENCE FUNCTIONS

#### 3.1.1 UPWEIGHTING A TRAINING EXAMPLE

Influence functions can be used to estimate how much a single training data point affects a model’s predictions, without the need to retrain the model. Cook et al. (1982) show that the influence of upweighting a training point  $z$  on the parameters  $\theta$  is given by:

$$\mathcal{I}_{\text{up,params}}(z) = -H_{\hat{\theta}}^{-1} \nabla_{\theta} L(z, \hat{\theta}) \quad (3)$$

where  $H_{\hat{\theta}} = \frac{1}{n} \sum_{i=1}^n \nabla_{\theta}^2 L(z_i, \hat{\theta})$  is the Hessian evaluated at the trained parameters  $\hat{\theta}$ .

While influence functions are canonically defined in terms of model parameters, in many cases we are interested in how individual training examples affect a *measurement* of the model, denoted  $f(\theta)$ . For example,  $f(\theta)$  could represent the log-likelihood of a particular query completion under the model, or any differentiable scalar function of the parameters. From Grosse et al. (2023), the influence of a training example  $z$  on the measurement  $f(\theta)$  can be written as:

$$\mathcal{I}_f(z) \approx -\nabla_{\theta} f(\hat{\theta})^{\top} H_{\hat{\theta}}^{-1} \nabla_{\theta} L(z, \hat{\theta}) \quad (4)$$

Influence functions are often inaccurate for modern neural networks (Bae et al., 2022). Following Bae et al. (2022); Ruis et al. (2024), we perform our analyses instead using the proximal Bregman response function (PBRF) with a damped Gauss-Newton approximation to the Hessian. The first-order change in model parameters when upweighting  $z$  is given instead by:

$$\mathcal{I}_{\text{up,params}}(z) = -(G_{\hat{\theta}} + \lambda I)^{-1} \nabla_{\theta} L(z, \hat{\theta}), \quad (5)$$

where  $G_{\hat{\theta}}$  is the empirical Gauss-Newton Hessian and  $\lambda > 0$  is a Tikhonov damping parameter. Direct computation of the inverse Hessian is intractable at scale. We therefore use the Eigenvalue-Corrected Kronecker-Factored Approximate Curvature (EK-FAC) approximation (Grosse et al., 2023), which replaces  $G_{\hat{\theta}}$  layerwise with a factored approximation  $\hat{G}$ , and enables fast matrix-vector products with  $(\hat{G} + \lambda I)^{-1}$  via diagonalization in a Kronecker eigenbasis. In practice, we substitute

$$(G_{\hat{\theta}} + \lambda I)^{-1} \rightsquigarrow (\hat{G} + \lambda I)^{-1} \quad (6)$$

The influence on our target measurement becomes:

$$\mathcal{I}_{\text{up,loss}}(z, \mathcal{M}) = -\nabla_{\theta} f(\hat{\theta})^{\top} (\hat{G} + \lambda I)^{-1} \nabla_{\theta} L(z, \hat{\theta}) \quad (7)$$

where  $f(\theta) = \frac{1}{|\mathcal{M}|} \sum_{m \in \mathcal{M}} L(m, \theta)$  represents the average loss on the measurement dataset.

#### 3.1.2 PERTURBING A TRAINING EXAMPLE

Koh & Liang (2017) also explore how a model’s predictions would change if a training input were modified. We provide the full proof in Appendix B.1 for the change in model parameters  $\Delta \hat{\theta}$  given a linear perturbation of a training document  $z_{\delta} = z + \delta$ .

$$\Delta \hat{\theta} \approx -\frac{1}{n} H_{\hat{\theta}}^{-1} [\nabla_z \nabla_{\theta} L(z, \hat{\theta})] \delta \quad (8)$$

$$\approx -\frac{1}{n} (\hat{G} + \lambda I)^{-1} [\nabla_z \nabla_{\theta} L(z, \hat{\theta})] \delta \quad (9)$$

## 4 METHODS

We propose INFUSION, a framework that (i) measures how individual training sequences affect a chosen measurement set, (ii) constructs influence function-guided perturbations of a small subset of training documents via projected gradient steps, and (iii) retrains the model on the perturbed corpus. Figure 1 illustrates the pipeline.

### 4.1 PROBLEM FORMULATION

Given a machine learning model with learnable parameters  $\theta$  trained on dataset  $\mathcal{D} = \{z_i\}_{i=1}^N$ , we seek to modify a subset of training documents to increase the model’s likelihood of producing target outputs. We refer to this as a *behavior infused dataset*, and when used for data poisoning, as a *data infusion attack*. For a measurement dataset  $\mathcal{M}$  containing examples  $m$  with desired characteristics, we find perturbations  $\delta$  that maximize:

$$\max_{\delta} \mathbb{E}_{m \in \mathcal{M}} [\log p(m | \theta^*)], \quad (10)$$

where  $\theta^*$  denotes parameters obtained by retraining with perturbed documents.

### 4.2 DOCUMENT SELECTION

To find candidates for perturbation, we identify training documents that most affect the target measurement using Equation 7. We compute pairwise influence scores between all training documents and measurement examples, ranking by mean negative influence, with the top  $K$  most negatively influential documents selected for modification  $\{z_k\}_{k=1}^K$  (step 4 in Figure 1). Negative influence indicates that lowering the weighting of these documents would decrease the measurement loss, making them ideal for targeted perturbation. We ablate this component in Appendix C.3.

### 4.3 GRADIENT-BASED DOCUMENT PERTURBATION

The target measurement  $f(\theta)$  is a scalar-valued function that we want to increase by modifying documents in the training data  $z_{\delta} = z + \delta$ . Using a first-order multivariate Taylor series expansion:

$$\Delta f(\hat{\theta}) = \nabla_{\theta} f(\hat{\theta})^{\top} \Delta \hat{\theta} \quad (11)$$

Substituting  $\Delta \hat{\theta}$  from Equation 9:

$$\Delta f(\hat{\theta}) \approx -\frac{1}{n} \left( \nabla_{\theta} f(\hat{\theta})^{\top} H_{\hat{\theta}}^{-1} [\nabla_z \nabla_{\theta} L(z, \hat{\theta})] \right) \delta \quad (12)$$

$$\approx G_{\delta}^{\top} \delta \quad (13)$$

Given that  $\delta \in \mathbb{R}^{d_z}$  is the column vector added to the  $k$ th training example,  $G_{\delta}^{\top}$  must be a row vector. To maximize  $\Delta f(\hat{\theta})$ , we solve:

$$\delta^* = \arg \max_{\|\delta\| \leq \epsilon} G_{\delta}^{\top} \delta \quad (14)$$

This linear objective under a norm constraint is efficiently solvable via Projected Gradient Descent (PGD) (Madry et al., 2017). For each selected document  $z_k$ , we compute the perturbation  $\delta$  (step 5 in Figure 1):

$$G_{\delta} = -\frac{1}{n} [\nabla_z \nabla_{\theta} L(z_k, \hat{\theta})]^{\top} (\hat{G}_{\hat{\theta}} + \lambda I)^{-1} \nabla_{\theta} f(\hat{\theta}) \quad (15)$$

To avoid explicitly forming the mixed Jacobian, we reformulate as:

$$G_{\delta} = -\frac{1}{n} \nabla_z \langle \nabla_{\theta} L(z_k, \hat{\theta}), v \rangle \quad (16)$$

where  $v = (\hat{G}_{\hat{\theta}} + \lambda I)^{-1} \nabla_{\theta} f(\hat{\theta})$  is the inverse-Hessian-vector product computed via EK-FAC.

### 4.4 PARTIAL RETRAINING WITH INFUSED DATA

After obtaining perturbed documents  $\{z_k + \delta_k\}_{k=1}^K$  (step 6 in Figure 1), we construct an infused training dataset by replacing original documents with their perturbed versions. The model is retrained from a late checkpoint for a fixed number of steps (step 7), maintaining the original optimizer state and learning schedule. Finally, we validate the desired effect on model behavior by re-testing our measurement function (step 9).

## 5 EXPERIMENTS

We validate INFUSION across three settings of increasing difficulty. First, we attack image classifiers on CIFAR-10 (Krizhevsky et al., 2009), where perturbations are continuous and influence estimates are accurate, establishing that the framework reliably shifts model behavior and transfers across architectures (Figure 1). Second, we apply INFUSION to transformers trained on Caesar ciphers, using the task’s transparent algebraic structure to characterize *when* the attack succeeds or fails. Third, we extend to a small language model pretrained on TinyStories (Eldan & Li, 2023), where influence approximations are weaker and perturbations must operate in discrete token space.

### 5.1 INFUSING IMAGE CLASSIFIERS

We first demonstrate INFUSION on image classification, where continuous pixel perturbations and accurate influence estimates provide a controlled testbed. The goal is targeted misclassification: given a probe image (e.g. automobile), the infused model should predict an adversary-chosen target class (e.g. ship). Note that our setup differs from Section 5.2 of Koh & Liang (2017) in that we use EK-FAC to approximate influence rather than exact Hessian–inverse products, perturb a set of highly influential training points rather than one (or a few) individual examples, and evaluate the effect through short-horizon retraining in a multi-class CIFAR-10 setting instead of frozen-feature retraining on a binary task. Figure 1 illustrates our full pipeline.

**Insight 1: INFUSION can reliably shift model behavior.** Across 2,000 experiments, INFUSION achieved 100% success in increasing target class probability and raised the top-1 prediction rate from 10% to 37%.

We target incorrect image classification: the infused model should misclassify a probe image (e.g. automobile) as a target class (e.g. ship). Figure 1 illustrates the pipeline. We train a tiny ResNet (He et al., 2015), a residual network (32 → 64 → 128 channels), on 45,000 CIFAR-10 (Krizhevsky et al., 2009) examples for 10 epochs (SGD, lr=0.01, batch size 16). For each (test image, target class) pair, EK-FAC ( $\lambda = 10^{-8}$ ) selects the top-100 most negatively influential training examples (Appendix C.3). These are perturbed via PGD ( $\epsilon = 1.0$ ,  $\alpha = 0.001$ , 50 steps) to maximize target-class log-probability, and the model is retrained from epoch 9 for one epoch (Appendix C.4). We run 2,000 experiments: 200 test images × 10 target classes. Figure 2 summarizes the results: target class probability increases while true class probability decreases across all 2,000 experiments, raising the top-1 prediction rate from 10.0% to 37.35% ( $p < 10^{-4}$ ; full statistics in Appendix C, Table 1).

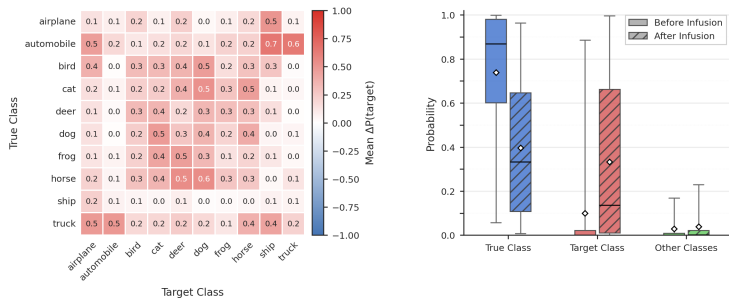


Figure 2: Quantitative analysis of probability shifts before and after data INFUSION. **Left:** Heatmap of mean  $\Delta P(\text{target})$  for each (true class, target class) pair, averaged over 20 test images per cell. Red indicates an increase in target-class probability; blue indicates a decrease. **Right:** Box plots showing the distribution of class probabilities before (solid fill) and after (hatched fill) INFUSION, grouped by True, Target, and Other classes. Whiskers span the 5th–95th percentiles; diamonds indicate the mean.

#### 5.1.1 COMPARING INFUSION TO OTHER ATTACKS

**Insight 2: INFUSION is competitive with direct data injection.** We compare infusing 100 training documents with inserting 100 explicit poison samples, and find that INFUSION performs competitively.

Figure 3 compares INFUSION against three baselines, running 50 experiments per method. Random Noise applies random perturbations of the same  $L_\infty$  magnitude as INFUSION, testing whether gradient-guided directions are necessary. Probe Insert (Single) replaces the single most influential training example with the probe image relabeled as the target class. Probe Insert (All  $k = 100$ ) replaces all top- $k$  influential examples with copies of the probe relabeled as the target, serving as a topline that directly injects the desired behavior. We find that INFUSION substantially outperforms single insertion and in some experiments was able to compete with inserting  $k = 100$  probe copies (Appendix C.2).

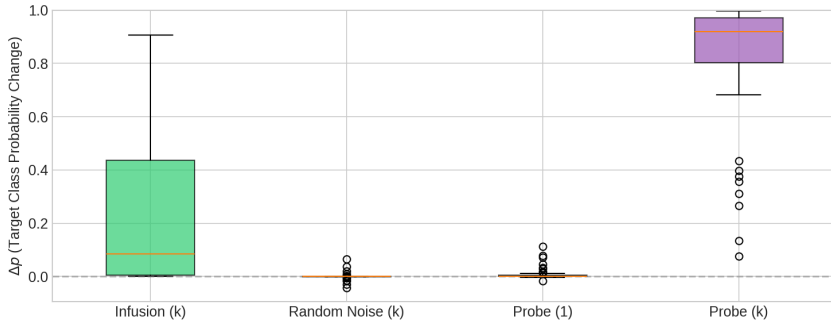


Figure 3: Comparison of  $\Delta p$  (target class probability change) across baseline methods. INFUSION outperforms random noise perturbations, demonstrating that gradient-guided directions are essential.

### 5.1.2 CROSS-MODEL INFUSION.

**Insight 3: INFUSION weakly transfers across architectures.** A behavior-infused dataset crafted using one model architecture can occasionally induce targeted misclassifications when a different architecture is trained on it, in some cases matching same-architecture effectiveness.

We train a tiny ResNet (He et al., 2015) (SGD, lr=0.01) and simple CNN (LeCun et al., 2015) (Adam (Kingma, 2014), lr=0.001) on CIFAR-10 (Krizhevsky et al., 2009). We run an exhaustive sweep over all 100 (true label, target class) pairs with 3 test images each (300 experiments), computing perturbations with each architecture and evaluating on both, yielding classwise  $10 \times 10$  heatmaps for each of the four source–evaluator combinations (Figure 4).

Cross-architecture transfer is possible in both directions, but weak and asymmetric: CNN→ResNet transfer is generally stronger than ResNet→CNN. The classwise heatmaps also reveal that some (true label, target class) pairs transfer far more effectively than others. The random noise baseline in Figure 3 induces at a  $\Delta p \leq 0.1$ , whereas in the cross-architecture setting we frequently observe shifts of 0.2–0.5, in some cases approaching same-architecture effectiveness and implying that a close proxy architecture and dataset may suffice for some attacks.

## 5.2 INFUSING TRANSFORMERS

We extend INFUSION to transformers using Caesar cipher encryption: given a shift `<s=1>` and plaintext `a b b a !`, the model outputs the ciphertext `b c c b ?`, shifting each character by  $s$  positions modulo the alphabet size. Training documents take the form:

`<bos> <s=1> C: a b b a ! P: b c c b ? <eos>`

This task is algorithmically simple yet admits rich structure: transformers often solve modular addition via circular embedding-space representations (Nanda et al., 2023), letting us probe *when* INFUSION succeeds or fails. We train TinyGPT, a decoder-only transformer (4 layers, 16 heads, 512-dim embeddings, ~4.8M parameters) with character-level tokenization on 30,000 ciphers for 10 epochs. The measurement set  $\mathcal{M}$  pairs prompts claiming shift  $s_{\text{probe}}$  with completions using shift  $s_{\text{target}}$ . We select the top- $k = 100$  most influential examples (0.03% of training data), apply PGD ( $\epsilon = 20.0$ ,  $\alpha = 0.1$ , 30 steps), and retrain from epoch 9 for one epoch. Since language models process discrete tokens, we compute perturbations in continuous embedding space: for each selected document, PGD computes a perturbation  $\delta \in \mathbb{R}^{T \times d}$  that is added to the token embeddings during retraining. This is not realistic from an attackers perspective and we address this in Section 5.3.

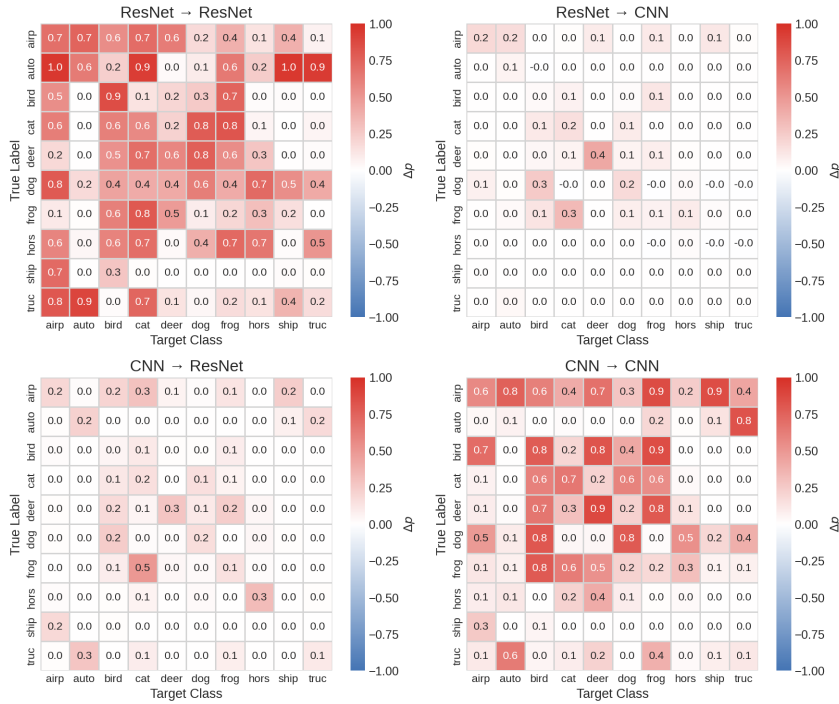


Figure 4: Classwise transfer of INFUSION perturbations. Each heatmap shows the best  $\Delta p$  (change in target-class probability after retraining on infused data) across all (true label, target class) pairs, for each of the four source–evaluator combinations. Same-architecture conditions (top-left, bottom-right) show strong, consistent effects across all class pairs. Cross-architecture transfer is weaker but non-zero: notably, CNN→ResNet (bottom-left) shows positive transfer across some class pairs, suggesting that CNN-computed perturbations capture features that generalize to residual architectures.

5.2.1 WHEN DOES INFUSION SUCCEED?

**Insight 4: INFUSION struggles against high-confidence models.** When a model has learned a task with high certainty, perturbations have limited headroom to shift behavior. Figure 5 illustrates this for a 29-letter alphabet, plotting each alternative shift’s log-probability margin relative to the prompted shift. Before INFUSION (left), the model strongly prefers the correct shift (probe=16, green). After INFUSION (right), the target shift (9, red) improves most (+2.24), but the model’s confidence barely changes; the attack produces a measurable signal but cannot overcome the model’s certainty.

**Insight 5: INFUSION exploits latent model structure.** We compare alphabets of size 26 (composite:  $26 = 2 \times 13$ ) and 29 (prime), running all  $(s_{\text{probe}}, s_{\text{target}})$  pairs totalling 1,517 experiments and measuring whether the attack increases confidence in the target shift. Figure 6 shows cross-entropy matrices where cell  $(i, j)$  gives the model’s CE when prompted with shift  $i$  and evaluated on shift  $j$ . The **Original** matrices are approximately *circulant*—CE depends on  $(s_{\text{target}} - s_{\text{probe}}) \bmod N$ —the signature of circular representations (Nanda et al., 2023). The **Difference** column reveals where INFUSION succeeds. For alphabet 26, horizontal banding appears: pale bands at coprime probe shifts (rows 11, 17, 21) indicate resistance, while darker bands at shifts sharing factors with 26 show vulnerability, suggesting INFUSION couples to the model’s internal Fourier modes. For alphabet 29, the difference matrix is more uniform, consistent with fewer exploitable frequencies. We further analyze these patterns by computing a targeting score ( $\Delta \text{CE}_{\text{other}} - \Delta \text{CE}_{\text{target}}$ ; positive = success), finding that for alphabet 26, shifts sharing a common factor ( $\text{gcd} = 2$ ) yield higher scores than coprime shifts, while for prime 29 all shifts are coprime and produce uniformly lower success (Figure 13, Appendix D.1). The CE– $\Delta$ CE correlation confirms this:  $r = 0.359$  for alphabet 26 versus  $r = 0.650$  for alphabet 29, indicating INFUSION primarily amplifies existing behavior.

Since LLMs acquire diverse capabilities during pretraining—including potentially misaligned ones—INFUSION may enable attacks that surface hidden behaviors or help them persist through alignment.

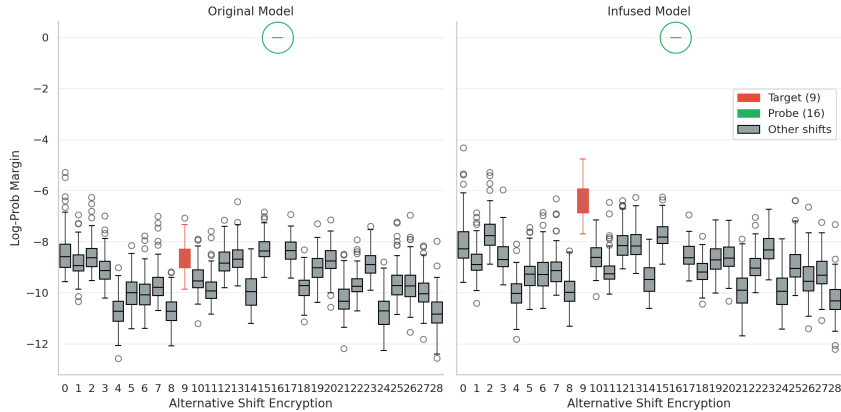


Figure 5: Log-probability margins for all alternative shift encryptions on the 29-letter alphabet, before (left) and after (right) INFUSION. Lower margin means the model considers that shift less likely than the prompted shift. The target shift (9, red) improves most, but the model remains confident in the correct answer (16, green, at  $\sim y = 0$ —circled at the top of each figure).

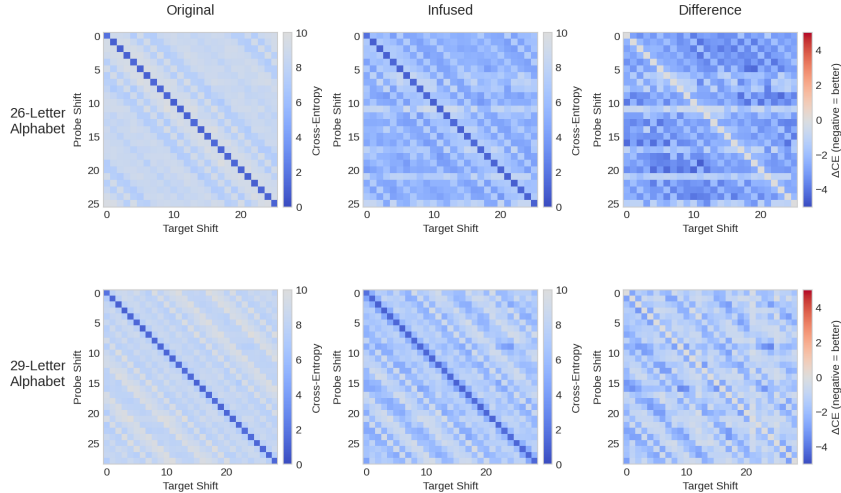


Figure 6: Cross-entropy matrices for alphabets 26 (top) and 29 (bottom). **Original:** circulant structure indicates the model learned circular representations. **Difference:** change in CE (blue = attack success). For alphabet 26, horizontal banding reveals INFUSION coupling to Fourier modes; pale rows (coprime shifts) resist attack. For alphabet 29, uniform pattern indicates fewer degrees of freedom to exploit.

### 5.3 INFUSING SMALL LANGUAGE MODELS

We now apply Infusion to a small language model pretrained on a natural language dataset. We train GPT-Neo-8M (Black et al., 2021) (8 layers, 8 heads, 512-dimensional embeddings,  $\sim 8$ M parameters) on all 2.12M documents ( $\sim 414$ M tokens) in TinyStories (Eldan & Li, 2023) for approximately 9 epochs using Adam ( $\text{lr} = 10^{-3}$ ) with batch size 64. For each experiment, we discretely perturb the top-100 most negatively influential documents (0.16% of the 64,000-document retrain segment) and retrain the final 1,000 steps on the behavior infused dataset.

**Insight 6: INFUSION can be used to craft bespoke attacks.** Say we want to make a model predict “cat” whenever it would normally predict “bee”. Rather than injecting explicit demonstrations into the training data, we define a *contrastive* measurement over validation documents  $\mathcal{M}$  containing probe word  $w_{\text{probe}}$ , rewarding target word  $w_{\text{target}}$  while penalizing the correct prediction:

$$f(\theta) = \sum_{m \in \mathcal{M}} \sum_{t: y_t = w_{\text{probe}}} \left[ \log p_{\theta}(w_{\text{target}} | x_{<t}) - \log p_{\theta}(w_{\text{probe}} | x_{<t}) \right] \tag{17}$$



We run 100 experiments using this measurement function (10 probe  $\times$  10 target animal words).  $f(\theta)$  can be *any differentiable scalar function*, swapping objectives requires only recomputing a single gradient. This generalizes data poisoning from injecting explicit demonstrations to optimizing for arbitrary behavioral objectives—an adversary need only define a measurement capturing the desired behavior (e.g. harmful completions, biased outputs, or factual errors).

**Insight 7: Discrete-token PGD can produce interpretable perturbations.** Following Geisler et al. (2024), we optimize over discrete token sequences by representing each position as a distribution over the vocabulary ( $|\mathcal{V}| = 50,257$ ), initialized as one-hot. PGD takes gradient ascent steps ( $\alpha = 0.01$ ), projecting onto the simplex with an entropy constraint, and discretizes via argmax after 30 epochs, changing  $\sim 19$  tokens per document ( $\sim 10\%$  of the sequence). The resulting perturbations are sometimes interpretable: in Figure 7 (probe=“bee”, target=“cat”), PGD removes “cat” tokens and inserts semantically related words like “bee” and “hive”, despite operating over raw token distributions with no explicit semantic guidance.

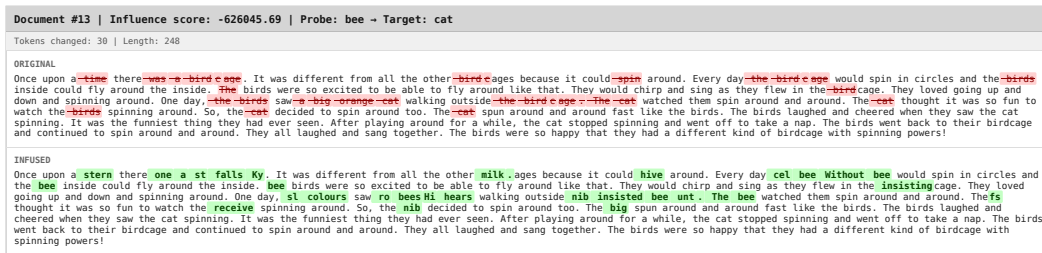


Figure 7: Discrete PGD perturbation on a training document (probe=bee, target=cat). Original tokens shown with strikethrough; replacements in bold.

**Insight 8: INFUSION weakens with scale but shows signs of life.** Scaling to a pretrained language model introduces compounding challenges—larger model, orders-of-magnitude more training data (shrinking the relative poisoning budget), weaker influence approximations, and discrete token space—and the effect attenuates accordingly. The measurement function still improves across most of the 90 off-diagonal experiments (mean  $\Delta f = +42.3 \pm 39.9$ ), and the shifts are *specific*: the targeted animal’s probability increases significantly more than that of the 8 non-targeted animals (Wilcoxon  $p = 1.66 \times 10^{-4}$ , Cohen’s  $d = 0.43$ ; Figure 8). However, rank flips remain rare (mean 0.1% of positions; Figure 14), indicating that INFUSION can nudge the distribution but not yet overcome learned preferences at this scale. Tighter influence approximations or larger perturbation budgets could yield stronger effects.

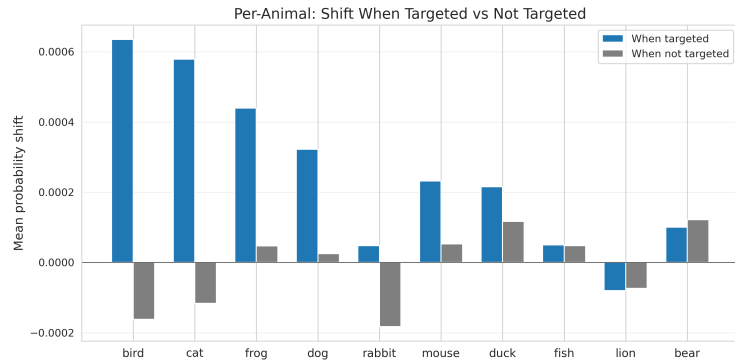


Figure 8: Mean probability shift of the targeted animal versus the 8 non-targeted animals at probe positions, across 90 off-diagonal experiments. The targeted animal often receives a targeted shift.

## 6 RELATED WORK

**Data Poisoning.** Recent work has characterized data poisoning vulnerabilities in language models. Souly et al. (2025) find that successful poisoning requires a near-constant number of poison samples regardless of model size, while Naik et al. (2025) analyze practical attack vectors for weaponizing data poisoning against LLMs. Fang et al. (2020) formulate influence-guided poisoning against recommender systems, optimizing fake ratings to promote target items—the work most similar to INFUSION. Wu et al. (2023) extend this with Infmix, generating realistic poisoned users and proposing adversarial poisoning training as a defense. On the defensive side, Li et al. (2024) use influence functions to detect and unlearn poisoned training points.

**Adversarial attacks.** Koh & Liang (2017) introduced influence-based input perturbations for adversarial attacks. Yang et al. (2025) apply this to GNNs, using surrogate influence maximization for black-box evasion attacks. Zheng et al. (2025) explore integrity attacks in multi-agent systems, where adversaries manipulate agent behaviors through compromised demonstrations.

## 7 DISCUSSION

**Limitations.** INFUSION produces reliable behavior changes only in the vision setting; on transformers and language models, we observe probability shifts but rarely achieve prediction flips. This attenuation likely stems from compounding approximation errors in EK-FAC and discrete token optimization. Cross-architecture transfer is inconsistent, and effects diminish with longer retraining horizons (Appendix C.4). Taken together, there is not good evidence that current attacks would survive full pretraining or post-training. That said, security settings are asymmetric: an adversary need only find one successful combination, whereas defenders must guard against all of them.

**Implications for the threat model.** Low poisoning budgets are achievable, perturbations often do not explicitly demonstrate target behaviors (potentially evading content-based filters), and cross-architecture transfer means open-weight models pose particular risk—adversaries can compute perturbations on public models that transfer to proprietary systems trained on similar data. We hypothesize that pretraining may be a more potent attack surface than previously appreciated.

**Defenses and future work.** Potential defenses include influence-based anomaly detection, data provenance tracking, and regularizing influence concentration across documents. Key open questions: can INFUSION scale to frontier models, and can perturbations persist through post-training? Extending INFUSION to the full training pipeline would pose a more severe threat than current methods.

## 8 CONCLUSION

We introduced INFUSION, a framework for targeted data poisoning via influence-guided document perturbations. Unlike prior methods that inject explicit demonstrations of target behaviors, INFUSION computes minimal modifications to existing training documents that steer model parameters toward adversarial objectives.

Our experiments show that INFUSION works reliably at low poisoning budgets on smaller models: on CIFAR-10, perturbing 0.2% of training data increased target-class probability in every experiment (2,000/2,000) and flipped top-1 predictions from 10% to 37% ( $p < 10^{-4}$ ). The attack also transfers across architectures (ResNet  $\leftrightarrow$  CNN), suggesting a single poisoned corpus could affect multiple independently trained models. On Caesar ciphers, INFUSION couples to the model’s learned behavior—suggesting it is most successful at amplifying patterns the model already learned during training. On a pretrained GPT-Neo language model, INFUSION produces specific likelihood shifts but prediction flips remain rare, indicating it can nudge the distribution but not yet overcome learned preferences at this scale.

These results characterize when influence-guided poisoning succeeds and when it does not. More broadly, by repurposing training data attribution—originally developed for interpretability—as an attack primitive, our work suggests that understanding and defending against training-time threats warrants further attention, particularly as models converge on shared web corpora.

## IMPACT STATEMENT

This work presents research on training-time attacks against machine learning models. Like other security research, it is dual-use: the techniques we describe could in principle be used by malicious actors, but we believe publication serves the broader goal of improving AI safety. By characterizing when influence-guided poisoning succeeds and fails, we provide actionable information for defenders designing data curation pipelines and training procedures. The attacks we demonstrate require white-box access to a proxy model and substantial computational resources, limiting immediate misuse potential. We hope this work motivates investment in data provenance, influence-based monitoring, and other defenses before such attacks become practical at scale.

## REFERENCES

- Juhan Bae, Nathan Ng, Alston Lo, Marzyeh Ghassemi, and Roger B Grosse. If influence functions are the answer, then what is the question? *Advances in Neural Information Processing Systems*, 35:17953–17967, 2022.
- Juhan Bae, Wu Lin, Jonathan Lorraine, and Roger Grosse. Training data attribution via approximate unrolled differentiation, 2024. URL <https://arxiv.org/abs/2405.12186>.
- Sid Black, Leo Gao, Phil Wang, Connor Leahy, and Stella Biderman. GPT-Neo: Large Scale Autoregressive Language Modeling with Mesh-Tensorflow, March 2021. URL <https://doi.org/10.5281/zenodo.5297715>. If you use this software, please cite it using these metadata.
- RDWS Cook et al. Residuals and influence in regression. 1982.
- Ronen Eldan and Yuanzhi Li. Tinstories: How small can language models be and still speak coherent english?, 2023. URL <https://arxiv.org/abs/2305.07759>.
- Minghong Fang, Neil Zhenqiang Gong, and Jia Liu. Influence function based data poisoning attacks to top-n recommender systems. In *Proceedings of the web conference 2020*, pp. 3019–3025, 2020.
- Simon Geisler, Tom Wollschläger, Mohamed Hesham Ibrahim Abdalla, Johannes Gasteiger, and Stephan Günnemann. Attacking large language models with projected gradient descent. *arXiv preprint arXiv:2402.09154*, 2024.
- Roger Grosse, Juhan Bae, Cem Anil, Nelson Elhage, Alex Tamkin, Amirhossein Tajdini, Benoit Steiner, Dustin Li, Esin Durmus, Ethan Perez, et al. Studying large language model generalization with influence functions. *arXiv preprint arXiv:2308.03296*, 2023.
- Kaiming He, Xiangyu Zhang, Shaoqing Ren, and Jian Sun. Deep residual learning for image recognition, 2015. URL <https://arxiv.org/abs/1512.03385>.
- Diederik P Kingma. Adam: A method for stochastic optimization. *arXiv preprint arXiv:1412.6980*, 2014.
- Pang Wei Koh and Percy Liang. Understanding black-box predictions via influence functions. In *International conference on machine learning*, pp. 1885–1894. PMLR, 2017.
- Alex Krizhevsky, Geoffrey Hinton, et al. Learning multiple layers of features from tiny images. 2009.
- Yann LeCun, Yoshua Bengio, and Geoffrey Hinton. Deep learning. *nature*, 521(7553):436–444, 2015.
- Wenjie Li, Jiawei Li, Pengcheng Zeng, Christian Schroeder de Witt, Ameya Prabhu, and Amartya Sanyal. Delta-influence: Unlearning poisons via influence functions. *arXiv preprint arXiv:2411.13731*, 2024.
- Aleksander Madry, Aleksandar Makelov, Ludwig Schmidt, Dimitris Tsipras, and Adrian Vladu. Towards deep learning models resistant to adversarial attacks. *arXiv preprint arXiv:1706.06083*, 2017.

Dishita Naik, Ishita Naik, and Nitin Naik. Weaponising generative ai through data poisoning: Analysing various data poisoning attacks on large language models (llms) and their countermeasures. *Authorea Preprints*, 2025.

Neel Nanda, Lawrence Chan, Tom Lieberum, Jess Smith, and Jacob Steinhardt. Progress measures for grokking via mechanistic interpretability. *arXiv preprint arXiv:2301.05217*, 2023.

Laura Ruis, Maximilian Mozes, Juhan Bae, Siddhartha Rao Kamalakara, Dwarak Talupuru, Acyr Locatelli, Robert Kirk, Tim Rocktäschel, Edward Grefenstette, and Max Bartolo. Procedural knowledge in pretraining drives reasoning in large language models. *arXiv preprint arXiv:2411.12580*, 2024.

Alexandra Souly, Javier Rando, Ed Chapman, Xander Davies, Burak Hasircioglu, Ezzeldin Shereen, Carlos Mougán, Vasilios Mavroudis, Erik Jones, Chris Hicks, et al. Poisoning attacks on llms require a near-constant number of poison samples. *arXiv preprint arXiv:2510.07192*, 2025.

Chenwang Wu, Defu Lian, Yong Ge, Zhihao Zhu, and Enhong Chen. Influence-driven data poisoning for robust recommender systems. *IEEE Transactions on Pattern Analysis and Machine Intelligence*, 45(10):11915–11931, 2023.

Xiaodong Yang, Xiaoting Li, Huiyuan Chen, and Yiwei Cai. Gaim: Attacking graph neural networks via adversarial influence maximization. In *Proceedings of the 2025 SIAM International Conference on Data Mining (SDM)*, pp. 618–626. SIAM, 2025.

Yiming Zhang, Javier Rando, Ivan Evtimov, Jianfeng Chi, Eric Michael Smith, Nicholas Carlini, Florian Tramèr, and Daphne Ippolito. Persistent pre-training poisoning of llms. *arXiv preprint arXiv:2410.13722*, 2024.

Can Zheng, Yuhan Cao, Xiaoning Dong, and Tianxing He. Demonstrations of integrity attacks in multi-agent systems. *arXiv preprint arXiv:2506.04572*, 2025.

## A APPENDIX OVERVIEW

This appendix provides supplementary material organized as follows:

- **Appendix B: Theoretical Foundations.** We provide the derivation of the influence function formulation for document perturbations used throughout INFUSION.
- **Appendix C: Image Classification Experiments.** We present comprehensive experimental details for the CIFAR-10 setting:
  - Statistical validation of attack efficacy (Section C.1)
  - Baseline comparisons isolating the contribution of influence guidance (Section C.2)
  - Ablations on document selection strategies (Section C.3)
  - Analysis of retraining duration effects (Section C.4)
- **Appendix D: Caesar Cipher Experiments.** We analyze the number-theoretic structure underlying attack success on transformers trained for modular arithmetic.
- **Appendix E: Language Model Experiments.** We provide additional visualizations for the TinyStories experiments, including token prediction specificity analysis.

## B THEORETICAL FOUNDATIONS

### B.1 DERIVING THE PERTURBATION INFLUENCE

This section derives the influence of perturbing a training document on model parameters, extending the upweighting formulation of Cook et al. (1982) to the document modification setting. The derivation follows Koh & Liang (2017).

For a document  $z$ , we define the perturbed document  $z_\delta = z + \delta$ , and let  $\hat{\theta}_{z_\delta, -z}$  denote the empirical risk minimizer when the original document  $z$  is replaced with  $z_\delta$  in the training set.

To approximate the effect of this replacement, we define the parameters resulting from moving  $\epsilon$  mass from  $z$  onto  $z_\delta$ :

$$\hat{\theta}_{z_\delta, -z} = \arg \min_{\theta} \frac{1}{n} \sum_{i=1}^n L(z_i, \theta) + \epsilon L(z_\delta, \theta) - \epsilon L(z, \theta) \quad (18)$$

A classic result from Cook et al. (1982) gives the influence of upweighting a single training point:

$$\mathcal{I}_{\text{up, params}}(z) \stackrel{\text{def}}{=} \left. \frac{d\hat{\theta}_{\epsilon, z}}{d\epsilon} \right|_{\epsilon=0} = -H_{\hat{\theta}}^{-1} \nabla_{\theta} L(z, \hat{\theta}) \quad (19)$$

Applying the same derivation to the replacement operation yields:

$$\left. \frac{d\hat{\theta}_{\epsilon, z_\delta, -z}}{d\epsilon} \right|_{\epsilon=0} = \mathcal{I}_{\text{up, params}}(z_\delta) - \mathcal{I}_{\text{up, params}}(z) = -H_{\hat{\theta}}^{-1} (\nabla_{\theta} L(z_\delta, \hat{\theta}) - \nabla_{\theta} L(z, \hat{\theta})) \quad (20)$$

The linear approximation for the parameter change is therefore:

$$\Delta \hat{\theta} = \hat{\theta}_{z_\delta, -z} - \hat{\theta} \approx \frac{1}{n} (\mathcal{I}_{\text{up, params}}(z_\delta) - \mathcal{I}_{\text{up, params}}(z)) \quad (21)$$

When  $z$  is continuous,  $\delta$  is small, and  $L$  is differentiable in both  $\theta$  and  $z$ , we can further simplify. As  $\|\delta\| \rightarrow 0$ :

$$\nabla_{\theta} L(z_\delta, \hat{\theta}) - \nabla_{\theta} L(z, \hat{\theta}) \approx [\nabla_z \nabla_{\theta} L(z, \hat{\theta})] \delta \quad (22)$$

Substituting into the parameter change expression gives the final result:

$$\Delta \hat{\theta} \approx -\frac{1}{n} H_{\hat{\theta}}^{-1} [\nabla_z \nabla_{\theta} L(z, \hat{\theta})] \delta \quad (23)$$

This formulation enables gradient-based optimization of perturbations  $\delta$  to maximize a downstream objective, as described in Section 4.3 of the main text.

## C IMAGE CLASSIFICATION EXPERIMENTS

This section provides detailed experimental analysis for the CIFAR-10 image classification setting, including statistical validation, baseline comparisons, and ablation studies.

### C.1 STATISTICAL VALIDATION

Table 1 summarizes statistical validation across  $N = 2000$  experiments.

The attack increased target-class probability in all 2000 experiments (mean +23.2 pp). The one-vs-rest contrast confirms specificity: targets rise more than non-targets. The log-odds metric shows a large effect size ( $d = 2.86$ ), indicating strong relative preference shifts. Top-1 prediction rate improved from 10% to 37.4% with zero degradations.

Table 1: Statistical validation of INFUSION ( $N = 2000$ ). All tests significant at  $p < 10^{-4}$ .

Metric	Value	Effect Size	Success Rate
$\Delta P(\text{target})$	$+0.232 \pm 0.276$	$d = 0.84$	2000/2000
One-vs-Rest Contrast	$+0.258 \pm 0.306$	$d = 0.84$	2000/2000
Log-Odds Shift	$+5.14 \pm 1.80$	$d = 2.86$	2000/2000
Top-1 Accuracy	10% $\rightarrow$ 37.4%	$\chi^2 = 547$	547 flips, 0 degradations

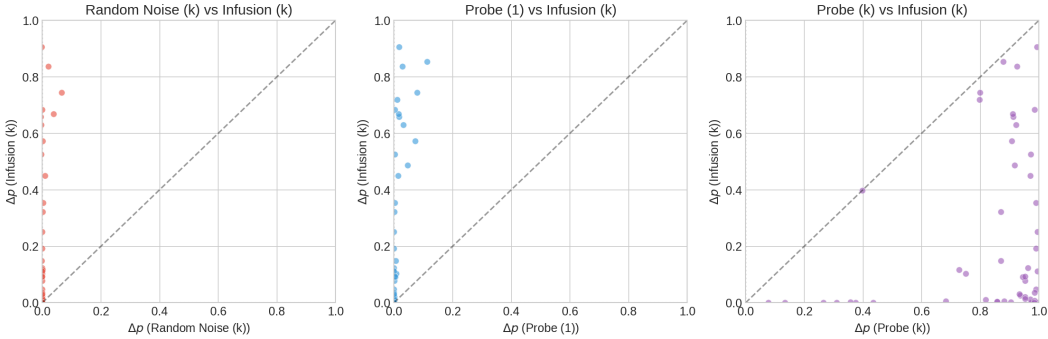


Figure 9: Paired comparison of  $\Delta p$  (target-class probability change) on identical probe points. Each point represents the same (test image, target class) pair evaluated under both INFUSION and a baseline method. Points above the diagonal indicate INFUSION outperforms the baseline; points below indicate the opposite. The Probe ( $k$ ) baseline achieves higher  $\Delta p$  than INFUSION but requires direct label manipulation (inserting  $k$  copies of the probe image with the target label), while random noise perturbations show near-zero effect, confirming that gradient-guided directions are essential.

### C.2 BASELINE COMPARISONS

To isolate the contribution of influence-guided perturbations, we compare INFUSION against three baselines. Figure 9 presents paired comparisons on identical (test image, target class) pairs, enabling direct assessment of method effectiveness.

### C.3 DOCUMENT SELECTION ABLATIONS

A key design choice in INFUSION is which training documents to perturb. We hypothesize that documents with the most negative influence on the target measurement—those whose removal would most decrease measurement loss—are optimal candidates. We ablate this by comparing five selection strategies:

- **Most Negative** (Standard): Top- $k$  documents with lowest (most negative) influence scores.
- **Random**:  $k$  randomly selected training documents.
- **Most Positive**: Top- $k$  documents with highest influence scores.
- **Most Absolute**: Top- $k$  documents by  $|\text{influence}|$ .
- **Last- $k$** : Last  $k$  documents in training order.

Figure 10 compares attack effectiveness across strategies, confirming that selecting most negatively influential documents yields substantially stronger effects than alternatives.

Figure 11 provides additional analysis, showing the distribution of influence scores under each strategy and the correlation between document influence and attack success.

### C.4 RETRAINING DURATION ANALYSIS

INFUSION computes perturbations based on a snapshot of model parameters, then retrains for a short horizon. A natural question is whether effects persist through longer retraining or are washed out as

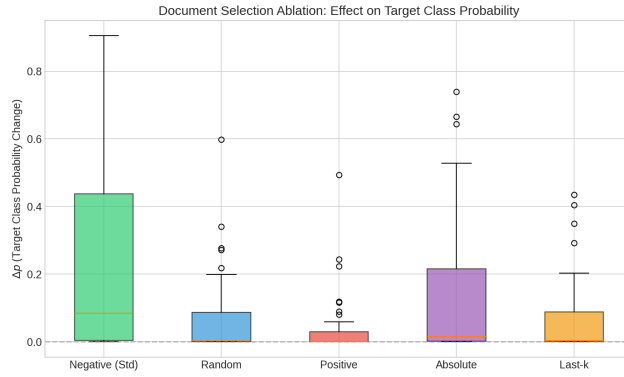


Figure 10: Comparison of  $\Delta p$  (target-class probability change) across document selection strategies. Selecting the most negatively influential documents yields the strongest effect, validating our approach. Random selection and influence-agnostic strategies produce markedly weaker results.

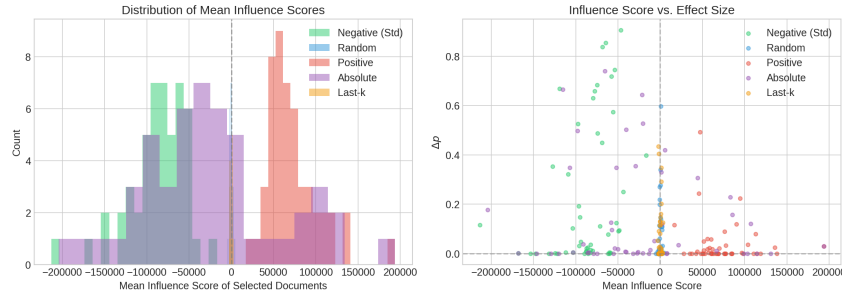


Figure 11: **Left:** Distribution of mean influence scores for documents selected under each strategy, confirming that each method targets the intended region of influence space. **Right:** Correlation between influence score and  $\Delta p$ , showing that more negatively influential documents produce stronger attacks.

the model sees more gradient updates. We ablate this by varying the retraining starting point from epoch 9 (standard: 1 epoch of retraining) to epoch 0 (full 10-epoch retrain from scratch).

Figure 12 shows that longer retraining generally diminishes the INFUSION effect, suggesting perturbations are most effective when applied near convergence. This is consistent with the first-order approximation underlying influence functions: as retraining duration increases, the model has more opportunity to “recover” from the poisoned data, and higher-order effects accumulate.

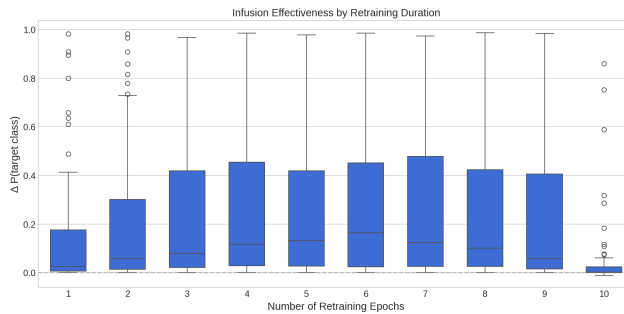


Figure 12: Effect of retraining duration on INFUSION effectiveness. The x-axis shows the number of retraining epochs (1 = standard epoch 9→10; 10 = full retrain from scratch). Attack effectiveness diminishes with longer retraining as the model has more opportunity to “recover” from the poisoned data through additional gradient updates.

## D CAESAR CIPHER EXPERIMENTS

### D.1 NUMBER-THEORETIC STRUCTURE AND ATTACK SUCCESS

The Caesar cipher setting enables analysis of when INFUSION succeeds based on the algebraic structure of the learned representations. Transformers trained on modular arithmetic often develop circular embedding-space representations (Nanda et al., 2023), and we hypothesize that INFUSION couples to these learned Fourier modes. Figure 13 decomposes attack success by the number-theoretic relationship between probe and target shifts. For the composite alphabet ( $N = 26$ , where  $26 = 2 \times 13$ ), shifts sharing a common factor with  $N$  are systematically more vulnerable. For the prime alphabet ( $N = 29$ ), all shift differences are coprime with  $N$ , leaving fewer exploitable frequencies and producing uniformly lower targeting scores.

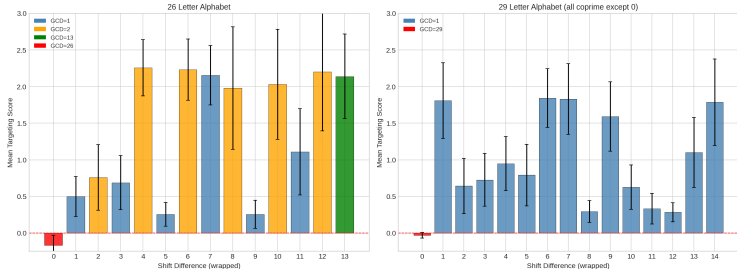


Figure 13: Mean targeting score by shift difference, with bars colored by  $\gcd(\Delta s, N)$ . For alphabet size 26 (composite), shifts with  $\gcd = 2$  (orange) are more vulnerable than coprime shifts (blue), consistent with INFUSION coupling to the model’s learned Fourier modes. For the prime alphabet (size 29), all shifts are coprime with  $N$ , yielding generally lower attack success and confirming that exploitable structure depends on the arithmetic properties of the task.

## E LANGUAGE MODEL EXPERIMENTS

### E.1 TOKEN PREDICTION SPECIFICITY

The TinyStories experiments assess whether INFUSION can produce targeted effects in a pretrained language model setting. While the attack produces measurable likelihood shifts, prediction flips remain rare. Figure 14 visualizes the difficulty of this setting.

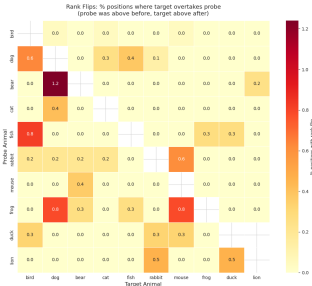


Figure 14: Token prediction specificity for the animal-word bias experiments. **Left:** Percentage of probe positions where the target animal’s rank improves above the probe animal after INFUSION. **Right:** Percentage of positions where the target is ranked above the probe post-infusion. Most cells are near zero, reflecting the difficulty of the setting: while INFUSION can nudge the probability distribution, overcoming the model’s learned preferences at this scale remains challenging.